Far infrared transmission of dielectrics at cryogenic and room temperatures: glass, Fluorogold, Eccosorb, Stycast, and various plastics

Mark Halpern, Herbert P. Gush, Edward Wishnow, and Vittorio De Cosmo

The absorption coefficient and index of refraction have been measured in the 2–30-cm^{-1} frequency range for the following materials at a temperature near 5 K: Pyrex, Fluorogold, Eccosorb CR110, Stycast 2850 FT, Plexiglas, TPX, Neoprene, Teflon, and Nylon. For some of these materials room temperature measurements were also made.

I. Introduction

As part of a program to build and calibrate a helium-cooled spectrometer to measure the submillimeter cosmic background spectrum, the absorption coefficient and index of refraction of several materials at a temperature near 5 K have been measured in the 2–30-wave number (cm^{-1}) range. These materials were candidates for either low-pass optical filters used to reduce the thermal radiation load on the detectors or absorbers to be used as low-temperature blackbody simulators. The optical properties of some of them at room temperature may be found in the literature, but low-temperature data are, in general, lacking. Where previous measurements are available they have been included for comparison.

II. Apparatus and Method

The layout of the optical components is shown in Fig. 1. They comprise a Barnes 600°C blackbody radiator, a dual input–dual output polarizing interferometer, and a monolithic silicon bolometer detector cooled to 4.2 K by liquid helium. The samples, placed just before the detector, were refrigerated by the same helium bath.

The interferometer is designed for use at 2 K in a sounding rocket and has been described elsewhere.[1] In these experiments it was mounted on an optical table and operated as a room temperature laboratory instrument. It functions in the rapid scan mode and generates double-sided interferograms every 1.7 s, from which spectra with an unapodized resolution limit of 0.46 cm^{-1} are obtained by a Fourier transform. The amplitude of the interferograms is proportional to the difference in brightness of the 600°C source in one entrance port of the interferometer and the room as seen by the other port. The throughput is set by the cold optics of the detector to be ~0.1 cm^2 sr. This is considerably below the throughput limit of the interferometer itself.

The radiation detector, kindly supplied by Rainer Weiss, is a monolithic silicon bolometer[2] mounted in a downward looking liquid helium cryostat which is sketched in Fig. 2. The field of view is defined by a copper condensing cone and a polyethylene lens mounted on the cold plate of the Dewar and by a diverging polyethylene lens which also serves as a room temperature vacuum window. A copper filter wheel is located below the cone–lens assembly so that any one of six samples can be placed in the optical path. The wheel is rotated by means of a belt made of Nylon fishing line wrapped around its rim and around a room temperature pulley. The filter wheel openings can be positioned in the beam with an accuracy of ±1° by measuring the resistance through a spring contact of a series of resistors soldered every 60° around the wheel. One of the resistors is an Allen Bradley 100-Ω 1/8-W carbon composition type which serves as a thermometer for the filter holder.

The low-frequency limit of the system's spectral response is determined by the condensing cone which has a waveguide cutoff at 2.3 cm^{-1}. The high-frequency limit set by the sampling interval is 235 cm^{-1}, but low-pass optical filters immediately in front of the detector block radiation of frequency higher than ~30

The authors are with the University of British Columbia, Physics Department, Vancouver, British Columbia V6T 2A6.

Received 19 October 1985.
0003-6935/86/040565-06$02.00/0.

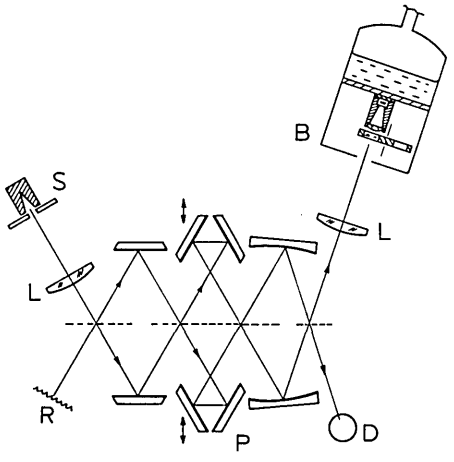

Fig. 1. Diagram of the optical system: P, a polarization interferometer (the dotted line represents wire grid polarizers, and the vertical arrows indicate the mirror movement altering the path difference); L, condensing lenses of TPX; S, a 600°C blackbody source; R, room at 23°C, a second blackbody radiation source; B, the liquid helium-cooled bolometer and sample wheel; and D, location of an optional detector not used for these measurements.

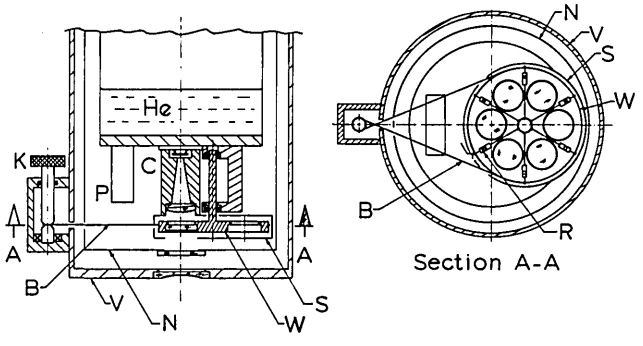

Fig. 2. Diagram of the detector Dewar: C, a condensing cone and monolithic silicon bolometer[2] fixed to the cold plate of a modified Infrared Laboratories liquid helium Dewar; P, a cooled preamplifier and load resistor; W, a copper wheel holding samples tied to the cold plate by a copper braid (not shown) and surrounded by the radiation shield S; K, a knob and shaft which drive the Nylon belt B by means of which the filter wheel is rotated; R, resistors to monitor the filter wheel position; N, the liquid nitrogen shield with a black polyethylene window; and V, the vacuum housing with a polyethylene window which acts as a diverging field lens.

cm^{-1}. These filters are selected for each experiment according to the sample under study to avoid large changes in the detector operating point when the incident radiation is reduced through insertion of cold samples into the beam.

In a typical sequence of measurements one of the six filter positions was left empty, usually the one corresponding to the resistance thermometer. A set of interferograms was recorded with the empty opening in the beam to furnish a reference spectrum. Then a data set was recorded for each of the five samples in the filter wheel, and finally another set of reference interferograms was collected. The data collecting phase of one complete experiment took ~15 min. If transmission spectra of samples at room temperature were desired, the samples were inserted in the beam immediately in front of the detector Dewar.

The bolometer signal, after suitable amplification and filtering was digitized with a 12-bit analog to digital converter triggered by pulses generated by a rotary position encoder on the drive shaft of the interferometer mirror carriage. Each interferogram consists of 1100 numbers, and a given measurement of a transmission spectrum consisted of 28 interferograms comprising about 45 s of integrating time. The data, recorded on magnetic tape, were transferred to the University's central computer for analysis. Complex Fourier transforms were calculated for each interferogram, and the effect of phase shifts caused by the detector and amplifier was removed. The resulting spectra were averaged for each sample. Transmission spectra were then obtained by taking the ratio of the averaged sample spectrum to the averaged reference spectrum. The ratio of two reference spectra measured on the same day was within 1–2% of unity over the major part of the spectral band.

The filter samples were in the form of flat disks a few millimeters thick or less, and therefore the transmission spectra display Fabry-Perot-type interference maxima and minima (channel spectra). The measured spectra were interpreted by comparing them to a theoretical expression for the transmission of a flat slab of absorbing dielectric. A computer graphics program overlayed the theoretical spectrum, broadened to simulate the finite resolution of the spectrometer, on the measured spectrum. A good visual fit was obtained by varying manually certain parameters (index, absorption coefficient) which enter the theoretical model. This method is more easily applied to the analysis of strongly absorbing samples than the technique developed by Loewenstein and co-workers[3] in their series of papers on optical constants in the far infrared, and it has the advantage that reflection spectra need not be measured.

The expression employed for the transmission is not found in the literature in a useful form, and it is now derived. In the standard waveguide analogy,[4] one can calculate the transmission of a slab of nonlossy dielectric of index n and thickness d, at a given frequency $\nu(\mathrm{cm}^{-1})$ given the admittance at the front surface:

$$Y(\nu) = n\left(\frac{\cos 2\pi n\nu d + jn \sin 2\pi n\nu d}{n \cos 2\pi n\nu d + j \sin 2\pi n\nu d}\right). \quad (1)$$

This quantity is equivalent to an index of refraction, and the electric field reflection coefficient is

$$\rho = \frac{1 - Y(\nu)}{1 + Y(\nu)}. \quad (2)$$

The power reflection and transmission coefficients are

$$R = \rho\rho^* \text{ and } T = 1 - R. \quad (3)$$

This treatment can be extended to the case of the lossy dielectrics by considering them poor conductors. It is useful to define a complex dielectric constant,

$$\epsilon_c = \epsilon\left(1 + \frac{\sigma}{j\omega\epsilon}\right), \quad (4)$$

where ϵ is the ordinary dielectric constant, and σ is the frequency-dependent conductivity. The form of Maxwell's equations is preserved,

$$\nabla \times \mathbf{H} = j\omega\epsilon_c \mathbf{E}, \tag{5}$$

and one can derive a complex admittance in the same way that Eq. (1) is obtained. The result is

$$Y(\nu) = \frac{1}{\eta'}\left(\frac{\eta' \cosh\gamma d + \sinh\gamma d}{\cosh\gamma d + \eta' \sinh\gamma d}\right), \tag{6}$$

where the complex wave vector is

$$\gamma = j\omega\sqrt{\mu\epsilon_c} = \alpha/2 + 2\pi j n\nu, \tag{7}$$

and the bulk impedance is

$$\eta' = \sqrt{\mu/\epsilon_c} = \frac{1}{n\sqrt{1 + \alpha/2\pi j n\nu}}. \tag{8}$$

The electric field reflection coefficient is given by Eq. (2). The coefficients for reflected and transmitted power are

$$R = \rho\rho^* \text{ and } T = \exp(-\alpha d)(1 - R). \tag{9}$$

Note that if α, the absorption coefficient, is set to zero, Eq. (6) reverts exactly to Eq. (1), the admittance for a lossless Fabry-Perot étalon.

The far right-hand sides of Eqs. (7) and (8) are valid under the assumptions that $\sigma/\omega\epsilon \ll 1$ and that $\mu = 1$. These assumptions are normally made for dielectrics, and we adopt them here. In fitting these expressions to the data it has also been assumed that the real part n of the index of refraction is constant in the frequency range examined and that the absorption coefficient varies with frequency as a power law: $\alpha = a\nu^b$. The materials have hence been characterized by the coefficients n, a, and b.

Strictly speaking, the real and imaginary parts of the index of refraction are connected by a dispersion relation. However, since here the object is to characterize filter materials by means of parameters useful in practice, a Kramers-Kronig analysis would be unnecessarily sophisticated, apart from being impractical, since a wide spectral range was not covered in these measurements.

Another approximation made was that the sample thickness was assumed in all cases to be the room temperature value. To have taken the contraction due to cooling into account would also have been an unnecessary refinement, since even for plastics the change in length going from 300 to 5 K is ~1%, which is the order of the accuracy in the determination, for example, of the parameter n. From a purely practical point of view, whether or not the various assumptions we have made are valid, the measured transmission spectrum of a sample of material can be reproduced from Eq. (6) using the room temperature thickness and the values of n and α which are reported here.

To illustrate the fitting procedure an example of the measured, and best-fit theoretical, spectra is shown in Fig. 3 for two thicknesses of Pyrex at a temperature of 4.8 K. For the thinner sample obvious Fabry-Perot fringes make clear the initial guess for n. For thick samples we do not resolve these fringes, and it is necessary to estimate n from the transmission extrapolated to zero frequency, which is the Fabry-Perot transmission spectrum averaged over frequency[5]:

$$\langle T \rangle = 2n/(n^2 + 1). \tag{10}$$

For nearly all materials measured, samples of several different thicknesses were used to make sure that the best fit parameters were independent of the sample geometry. This turned out to be the case except for Fluorogold as will be explained.

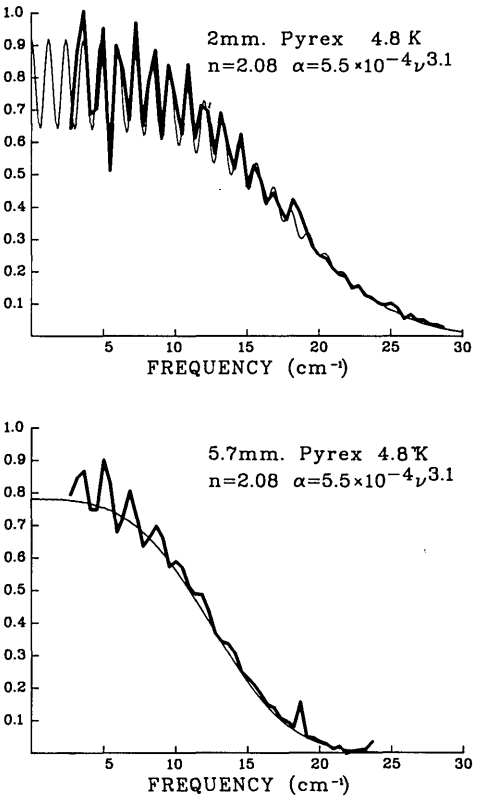

Fig. 3. Measured (heavy line) and fitted (light line) transmission curves for two thicknesses of Pyrex glass at a temperature near 5 K. The values of n and α listed are the parameters of the fitted curve. For the thinner sample Fabry-Perot interference maxima and minima (a channel spectrum) are clearly evident. For the thicker sample the channel spectrum is not resolved. The observed oscillations in that spectrum are due to optical coupling between the sample and detector cone assembly. These oscillations are also present in the upper spectrum. The peak at 18 cm^{-1} in both spectra is due to imperfect cancellation of a very strong water vapor absorption line.

III. Results

The results are presented numerically in Table I as a list of the best fit parameters n, a, and b. In addition, in Figs. 4, 5, and 6, the absorption coefficient $\alpha = a\nu^b$ is plotted on a log–log scale for most of the materials measured.

Figure 4 shows the data for glass and Fluorogold. A rather unexpected result is the significantly lower absorption at 5 K than at room temperature in both materials at frequencies below ~20 cm^{-1}. Near 30 cm^{-1}, on the other hand, the absorption seems to be

Table I. Best Fit Optical Parameters[1]

Material	Thickness (mm)	Temperature (kelvin)	Index n	Abs. coeff $\alpha = a\nu^b$ cm^{-1} a	b
Pyrex[2]	2.00	4.8	2.08	5.5×10^{-4}	3.1
Pyrex	2.80	4.8	2.08	5.5×10^{-4}	3.1
Pyrex	5.70	4.8	2.08	5.5×10^{-4}	3.1
Pyrex	2.00	300	2.11	8.5×10^{-2}	1.6
Schott glass[3]	2.10	4.8	2.08	1.5×10^{-4}	3.5
Cover slip[4]	0.22	4.8	2.42	6.5×10^{-4}	3.4
Fluorogold rod[5]	1.05	4.8	1.60	2.5×10^{-3}	3.6
Fluorogold rod	2.25	4.8	1.68	3.5×10^{-5}	3.6
Fluorogold rod	4.00	4.8	1.68	3.5×10^{-3}	3.6
Fluorogold rod	2.25	300	1.70	2.7×10^{-3}	2.4
Eccosorb CR110[6]	0.56	4.8	1.88	0.32	1.2
Eccosorb CR110	1.00	4.8	1.85	0.28	1.2
Eccosorb CR110	2.18	4.8	1.88	0.30	1.2
Eccosorb CR110	1.00	300	1.88	0.70	1.1
Eccosorb CR110	2.25	300	1.88	0.60	1.1
Stycast 2850 FT[6]	0.90	4.8	2.00	7.0×10^{-3}	2.2
	1.85	4.8	2.00	7.0×10^{-3}	2.2
	1.45	300	2.28	2.5×10^{-2}	2.2
Plexiglas[7]	0.83	4.8	1.53	9×10^{-3}	2.0
Plexiglas	1.35	4.8	1.60	9×10^{-3}	2.0
Plexiglas	1.35	300	1.60	2.5×10^{-2}	1.8
Plexiglas	3.15	300	1.60	2.5×10^{-2}	1.8
TPX sheet[8]	3.18	300	1.416	0.01	1.0
TPX sheet	6.50	300	1.42	0.01	1.0
TPX sheet	0.60	4.8	1.43	Low[9]	—
Neoprene sheet	1.75	4.8	2.4	0.6	1.2
Teflon	0.76	4.8	1.44	Low[9]	
Nylon[10]	1.6	4.8	1.72	5.0×10^{-4}	2.9

[1] Valid over the 2–30-cm^{-1} frequency range.
[2] Corning Glass Works, Corning, N.Y.
[3] Schott glass used as a replacement for Pyrex by our glassblower.
[4] Standard microscope cover slip.
[5] E.I. DuPont de Nemours & Co., Inc., Wilmington, DE.
[6] Emerson and Cuming, Gardena, CA.
[7] Rohm & Haas Canada, Ltd.
[8] Yarsley Research Laboratories Ltd., Slough, Bucks, U.K.
[9] Samples were too thin to show significant absorption ($\gtrsim$10%) up to the highest frequency measured, 40 cm^{-1}.
[10] Because of a malfunction, accurate absorption coefficients of Nylon were not obtained, and the figures given should be considered a general guide only to this rather strongly absorbing plastic.

temperature independent, a result consistent with previously reported high-frequency measurements in some other glasses.[6] The purpose in measuring the optical properties of Pyrex and other glasses at low temperatures was to evaluate their use in a 3 K blackbody radiation source with a small thermal time constant. Because Pyrex becomes more transparent in the frequency range of interest as it is cooled to cryogenic temperatures, a greater amount of material is required than was originally estimated for a satisfactory source. The construction of a blackbody simulator will be reported elsewhere. The rapid rise in absorption with frequency makes glass attractive as a low-pass optical filter in applications where the large thermal contraction, low thermal conductivity, or bulk of Fluorogold is inconvenient. Fluorogold has, however, lower reflection losses.

Fluorogold is a glass-filled Teflon, widely used as a cold low-pass filter in the far IR. The samples measured here were disks cut from rod stock in which the glass fibers are presumably predominantely aligned along the rod axis. These samples were measured to polarize $<\frac{1}{2}$% in contrast to disks cut from Fluorogold in sheet form which polarize ~7% as has been reported elsewhere.[7,8]

An unexpected feature of the results is that both the index of refraction and the absorption coefficient are lower for the thinnest sample of Fluorogold than for the thicker samples. It is believed that glass threads have been removed by cutting and machining the thin disk since a loss of absorber would produce these effects.

The index of refraction of a mixture of materials is obtained from the average polarizability,

$$n_F = [1 + 4\pi(P_T(1 - \delta) + \delta P_G)]^{1/2}, \quad (11)$$

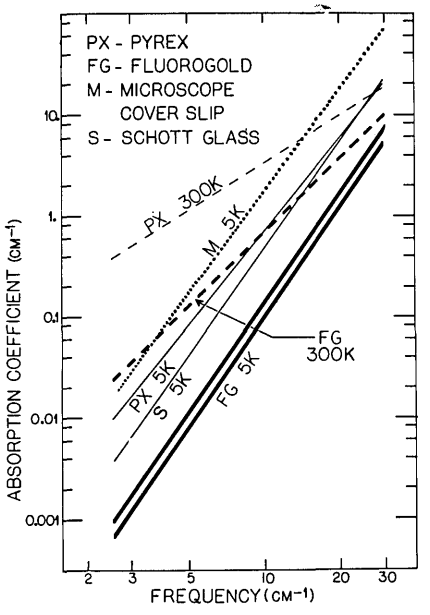

Fig. 4. Absorption coefficients as a function of frequency for Pyrex PX, a microscope cover slip M, a Schott glass S, and Fluorogold FG. The curves are plots of the best fit values of $\alpha = a\nu^b$ as per Table I. The lower of the two curves marked FG; 5 K is for a thin sample 1 mm thick. The smaller absorption coefficient than for thicker samples (upper curve) is probably due to a loss of glass filler during machining. Notice that at 30 cm^{-1} the absorption coefficients of Pyrex and Fluorogold do not vary with temperature.

$$n_F^2 - n_T^2 = \delta(n_G^2 - n_T^2). \tag{12}$$

where the subscripts F, T, and G stand for Fluorogold, Teflon, and glass, respectively, and δ is the concentration of glass. It may be derived from this expression that

Since we have measured n_F and n_T we can calculate $\delta\,(n_G^2 - n_T^2)$. The absorption coefficient of our thinnest sample is reduced by a factor of 0.71 from the bulk value. If this is due to the removal of some glass, δ would be reduced by this same factor. One would expect the index of the thin sample to be

$$n = \sqrt{n_T^2 + 0.71(n_F^2 - n_T^2)} = 1.61. \tag{13}$$

This is in good agreement with our measured value of 1.60 confirming the hypothesis that the composition of the thin sample has been modified.

Figure 5 shows the absorption coefficients for Stycast 2850 FT, and precast Eccosorb CR110, both products of Emerson Cuming, Inc. The former is a sapphire-filled epoxy commonly used for bonding metals at low temperature. The latter, which absorbs strongly in the microwave region, has been used to make submillimeter calibration sources.[9–12] Included in the figure for comparison purposes are recently published measurements by Hemmati *et al.*[12] and Peterson and Richards[11] on Eccosorb samples which they cast themselves. Hemmati *et al.* added a silicon powder to the mixture to inhibit settling of the iron filings during curing. In view of this difference in composition the difference in absorption coefficient is not unexpected. Our results approximately agree, on the other hand,

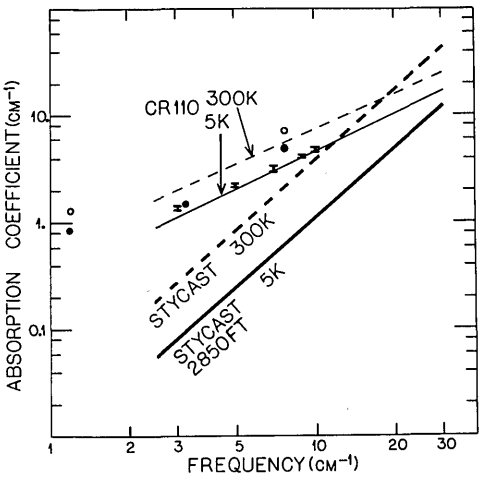

Fig. 5. Absorption coefficients of precast Eccosorb CR110 and Stycast 2850 FT. The error bar symbols show measurements at 2 K by Peterson and Richards[11] for CR110 which they cast themselves. The circles are measurements reported by Hemmati *et al.*[12] for CR110 mixed with CAB-O-SIL; open circles are room temperature results; filled circles are results at 80 K. Those authors saw no further change as their samples were cooled to 10 K.

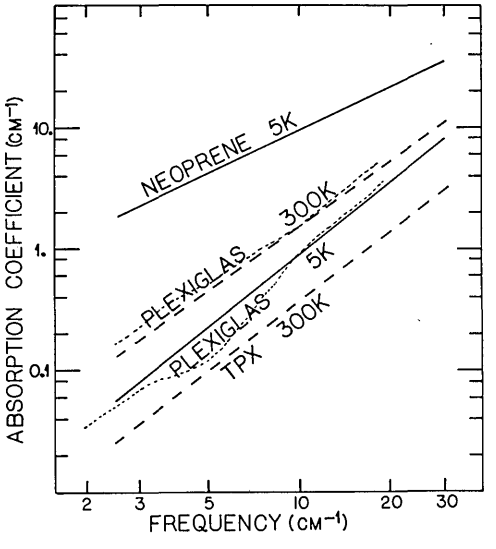

Fig. 6. Absorption coefficients of Neoprene, Plexiglas, and TPX. The fine dotted lines overlaying the Plexiglas curves are from previous work by Mon and Sievers.[14] The departure from a power law reported by them in the 3–8-cm^{-1} region would cause a change of <1 ½% in our measured transmission spectra. We lack the sensitivity to see this effect.

with those of Peterson and Richards.

Finally, Fig. 6 shows absorption curves for TPX, a commonly used far-IR window material,[13] Plexiglas, and Neoprene. Plexiglas is a candidate for a low-pass filter, having absorption properties similar to those of Fluorogold; it has the advantage that it is not polarizing but the disadvantage that the reflection loss is higher. The slight deviation from a power law between 3 and 8 cm^{-1} reported by Mon and Sievers[14] would change the transmission of our thickest sample by <1.5%. This effect is smaller than our uncertain-

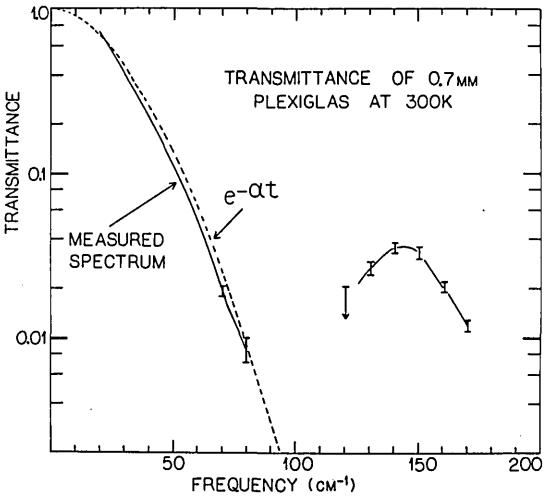

Fig. 7. Transmittance of room temperature Plexiglas showing a transmission window near 140 cm^{-1}. The solid line passes through the peaks of a resolved channel spectrum measured on a BOMEM FT spectrometer. The dashed curve shows the absorption losses extrapolated from the low-frequency results of Table I. Measurements of thinner samples confirmed that transmission in the high-frequency window scales properly with sample thickness.

ties. A transmission window at 140 cm^{-1} was discovered in room temperature Plexiglas in a measurement of the spectrum over a wide frequency range using a commercial BOMEM FT spectrometer. The spectrum is shown in Fig. 7. If Plexiglas is used as a low-pass filter, this window should be blocked.

Neoprene has a very high absorption coefficient and would be a good candidate for a low-temperature calibration source were it not for the high index of refraction and the difficulty of bonding it to a surface of well-defined temperature.

Some measurements were also made of Teflon and Nylon. The results are reported in Table I only. Teflon is essentially transparent up to 30 cm^{-1}, whereas Nylon displays a relatively strong absorption. It could be useful as a filter but not as a low-temperature blackbody simulator because of its very poor thermal conductivity.

This work was supported by a research grant from the Natural Sciences and Engineering Research Council of Canada.

References

1. H. P. Gush, "Rocket Measurement of the Cosmic Background Submillimeter Spectrum," in *Proceedings, 1983 Space Helium Dewar Conference*, J. B. Hendricks and G. R. Karr, Ed. (U. Alabama in Huntsville, 1984), p. 99.
2. P. M. Downey *et al.*, "Monolithic Silicon Bolometers," Appl. Opt. **23**, 910 (1984).
3. E. V. Loewenstein and D. R. Smith, "Optical Constants of Far IR Materials. 1: Analysis of Channeled Spectra and Application to Mylar," Appl. Opt. **10**, 577 (1971); E. V. Loewenstein, D. R. Smith, and R. L. Morgan, "Optical Constants of Far IR Materials. 2: Crystalline Solids," Appl. Opt. **12**, 398 (1973); D. R. Smith and E. V. Loewenstein, "Optical Constants of Far Infrared Materials. 3: Plastics," Appl. Opt. **14**, 1355 (1975).
4. S. Ramo and J. R. Whinnery, *Fields and Waves in Modern Radio* (Wiley, New York, 1953).
5. M. Born and E. Wolf, *Principles of Optics* (Pergamon, London, 1959), p. 326.
6. A. Hadni, J. Caludel, X. Gerbaux, G. Marlot, and J.-M. Munier, "Sur le Comportement différent des cristaux et des verres dans l'absorption de l'infrarouge lointain (40–1500 μm) à la température de l'hélium liquide," Appl. Opt. **4**, 487 (1965).
7. G. Dall'Oglio, P. De Bernadis, S. Masi, F. Melchiorri, A. Blanco, F. D'Allesandro, and S. Fonti, "Polarization Properties of Fluorogold in the Far Infrared," Infrared Phys. **22**, 185 (1982).
8. A. Blanco, S. Fonti, M. Mancarella, and V. De Cosmo, "Polarization Properties of Some Materials at Near Millimeter Wavelengths," Int. J. Infrared Millimeter Waves **4**, 751 (1983).
9. D. Muehlner and R. Weiss, "Balloon Measurements of the Far Infrared Background Radiation," Phys. Rev. D **7**, 326 (1973).
10. I. G. Nolt, J. V. Radostitz, P. Kittel, and R. J. Donnelly, "Submillimeter Detector Calibration with a Low Temperature Reference for Space Applications," Rev. Sci. Instrum. **48**, 700 (1977).
11. J. B. Peterson and P. L. Richards, "A Cryogenic Blackbody for Millimeter Wavelengths," Int. J. Infrared Millimeter Waves **5**, 1507 (1984).
12. H. Hemmati, J. C. Mather, and W. L. Eichhorn, "Submillimeter and Millimeter Wave Characterization of Absorbing Materials," Preprint.
13. G. W. Chantry, H. E. Evans, J. W. Fleming, and H. A. Gebbie, "TPX a New Material for Optical Components in the Far Infrared Spectral Region," Infrared Phys. **9**, 31 (1969).
14. K. K. Mon and A. J. Sievers, "Plexiglas: a Convenient Transmission Filter for the FIR Spectral Region," Appl. Opt. **14**, 1054 (1975).